C. R. Chimie 22 (2019) 96–102

Contents lists available at ScienceDirect

Comptes Rendus Chimie

www.sciencedirect.com

Account/Revue

Fe_3O_4 anodes for lithium batteries: Production techniques and general applications

Qichao Wu, Rongli Jiang*, Lixue Mu, Senyuan Xu

College of Chemical Engineering and Technology, China University of Mining and Technology, No. 1, Daxue Road, Xuzhou City 221116, Jiangsu Province, China

ARTICLE INFO

Article history:
Received 6 August 2018
Accepted 27 September 2018
Available online 29 October 2018

Keywords:
Lithium batteries
Iron oxides
Fe_3O_4 anode
Nanocomposites
Nanostructures

ABSTRACT

Iron oxides, such as Fe_3O_4, are putative anode materials for rechargeable lithium-ion batteries (LIBs). LIBs are extensively used as power sources for electronics. They typically consist of cells, with each cell built out of a lithium cathode and a graphite anode. However, graphite anodes suffer from the disadvantages of significant density, large volume, low energy density, and inferior safety levels. Iron oxides seem to be a promising substitute to the currently used graphite anodes due to their high capacity, extensive availability, good stability, and environmental tolerance. Nevertheless, several hurdles prevent their market expansion, such as inferior electronic/ionic conductivity, large volume changes, poor cycling performance, and low coulombic efficiency. Using Fe_3O_4 seems to be one alternative to address these challenges. This review will cover the current state of development of iron oxide electrodes with respect to design, production techniques, and general applications.

1. Introduction

Lithium-ion batteries (LIBs) are leading the digital revolution and are exclusively used in portable electronic devices. In addition, their usage is rapidly increasing for utility in electric vehicles. Overall, it is estimated that a demand of almost 100 Gigawatt hours (GWh) of LIBs is needed to cover the requirements for electric vehicles. In addition to that, they are also used to support the fluctuating green energy supply from renewable resources. Thus, LIBs constitute one of the most important factors of technology in the 21st century.

Typically, a LIB is constructed by connecting several lithium-ion (Li-ion) cells together in parallel, series, or using a combination of configurations to form a module that can be integrated to build a battery pack [1,2]. In turn, a Li-ion cell comprised a cathode, an anode, and an electrolyte [1]. The electrodes are segregated by means of a microporous polymer membrane that enables the exchange of Li ions when inhibiting electrons. The LIB operates through cycles of charging and discharging via a shuttle chair mechanism. Initially, the electrodes are linked to an external electrical source during charging and the cathode releases its electrons, which travel externally to the anode. Concurrently, the Li ions in the electrolyte move from the cathode to the anode internally. This mechanism allows the storage of electrochemical energy in the form of a difference in the chemical potential between the cathode and the anode. Throughout the discharging phase, the electrons travel back from the anode to the cathode via the external load, whereas Li ions travel from the anode to the cathode through the electrolyte.

The performance of LIBs depends on specific energy, specific capacity, cyclability, volumetric energy density, safety, robustness, and discharging–charging rate. Specific energy (Wh kg^{-1}) represents the energy that can be stored and released per unit mass and is calculated as a product of

* Corresponding author.
E-mail address: rongli_jiang@sina.com (R. Jiang).

https://doi.org/10.1016/j.crci.2018.09.016
1631-0748/

the specific capacity (Ah kg^{-1}) and operating voltage (V) [3]. The specific capacity, which represents the quantity of charge that can be stored per unit mass, is dependent upon the number of electrons evolved from the reactions and atomic mass of the electrode material [3]. Another parameter that could be used to estimate the performance abilities of LIBs is cyclability, which represents the reversibility of the Li-ion insertion. Furthermore, volumetric energy density (Wh L^{-1}) is defined as the power consumption of 1 W for 1 h per 1 L.

Various types of electrolytes and electrode materials have been explored as putative candidates for the fabrication of LIBs. Traditionally, the negative electrode was fabricated from carbon, the positive electrode was manufactured from a metal oxide such as $LiCoO_2$ or $LiFePO_4$, whereas the electrolyte consisted of a Li salt in an organic solvent. Alternative electrolyte materials such as polymer gels and ceramic electrolytes have also been reported. New approaches to designing the cathodes have been applied and different anode materials (e.g., Fe_3O_4) have been used. The focus of this review is the negative electrode materials, namely Fe_3O_4.

2. Fe_3O_4 anodes

Fe_3O_4 anodes represent an exciting alternative to traditionally used carbon anodes. Fe_3O_4 is characterized by high theoretical specific capacity (926 mAh g^{-1}), safety, superior conductivity, abundant supply, cost-effectiveness, and ecofriendliness. However, it suffers from the occurrence of large specific volume changes in the host matrices through different cycling phases, which can lead to pulverization of electrodes and rapid capacity decay. Another potential issue is the first cycle irreversibility that limits how LIBs can be manufactured, which had typically been performed in the discharged state. Ways to address these issues include changes in the manufacturing process of the anodes while also developing iron oxide–based nanostructures and iron oxide–based composites on conductive substrates. Specifically, to address these challenges, new manufacturing techniques and designs that have been used include electrospinning [4], liquid shear spinning, magnetic-spinning [5], and force spinning [6], in addition to sol–gel polymerization [7]. These methods result in structures that can be clustered into two groups: Fe_3O_4 nanostructures and Fe_3O_4 on conductive substrates or other stable metal oxides.

2.1. Production techniques for Fe_3O_4 anodes

In the following sections, two commonly used manufacturing techniques are described: electrospinning and sol–gel polymerization. After that, we will discuss different advancements in nanostructures and stable metal Fe_3O_4 combinations.

2.1.1. Electrospinning

One of the widely used methods that have been used in preparing Fe_3O_4 composite fibers for LIB electrodes is electrospinning [8], which is a flexible technique used in the fabrication of a range of materials. Some research groups modified this method for the fabrication of nanoscale electrostatic fibers by subjecting a polymer solution or a melt to a strong electric field (Fig. 1) [9,10]. The fibers produced by this process possess diverse characteristics such as high surface area to volume ratio, controllable porosity, high reversible capacity, superior capacity retention, and acceptable rate capability.

2.1.2. Sol–gel polymerization

Sol–gel technique is used to synthesize inorganic polymeric materials, in which molecular precursors are first dissolved in a liquid and then hydrolyzed to yield solid-in-liquid dispersions (sols). Then, a condensation reaction forms the solid network filled with liquid (gel). Interestingly, Fe_3O_4/Fe/carbon composites were fabricated through sol–gel polymerization followed by heat treatment [7]. The composite was in the form of a core–shell construction where homogeneous spherical Fe_3O_4/Fe nanoparticles of 100 nm are wrapped by an amorphous carbon matrix. This carbon matrix accommodates any volume expansion/contraction of Fe_3O_4 that could take place during discharge–charge cycles and also preserves the electrodes. The composite electrode exhibited a stable and reversible capacity, albeit with a modest value (600 mAh g^{-1} at a current of 50 mA g^{-1} between 0.002 and 3.0 V) (Fig. 2a). It is worth noting that the Fe_3O_4/Fe/carbon composite electrode reduces the risk of high-surface-area Li plating at the end of recharge owing to its slightly higher voltage plateau (Fig. 2b).

3. Fe_3O_4 nanostructures

3.1. Fabrication of Fe_3O_4 nanostructures

Nanostructure fabrication is one of the primary techniques to enhance the performance of the LIB electrodes. This approach has several advantages: (1) nanostructures possess short transport length that reduces the diffusion time of Li ions; (2) an increased electrode/electrolyte contact area that increases charge density; (3) strain can be significantly decreased during lithiation and dilithiation processes [11]; (4) protection of the structural integrity of the electrodes; and (5) maintain cycle performance. These advantages have led the way to various nanostructures (nanowires, nanotubes, nanowalls, nanosheets, and nanoparticles) being used to increase the effectiveness of Fe_3O_4 LIB electrodes [11,12]. Furthermore, to enhance the conductivities and decrease the diffusion length, Fe_3O_4 was integrated with a variety of metal nanostructures, polymers, and carbon materials.

3.1.1. Bicontinuous mesoporous Fe_3O_4 nanostructures grafted onto graphene foam

An interesting approach was reported by Luo et al. [11], where atomic layer deposition was performed to graft bicontinuous mesoporous Fe_3O_4 nanostructures on three-dimensional graphene foams (GFs). Atomic layer deposition has the ability to produce thin films for various types of materials with a high degree of conformity, thickness modulation, and film composition control [13]. The resulting composite (GF–Fe_3O_4) was directly used as a LIB

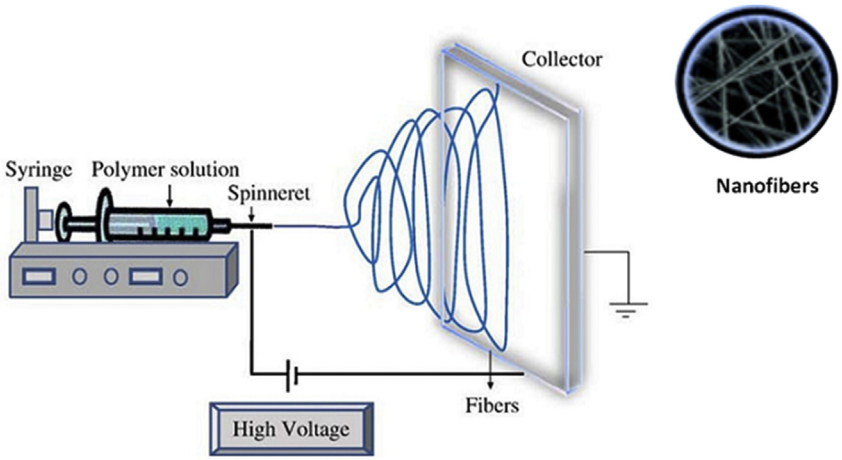

Fig. 1. A layout of the electrospinning workflow for the production of Fe_3O_4 electrodes for use in lithium batteries (adapted from Ref. [10]).

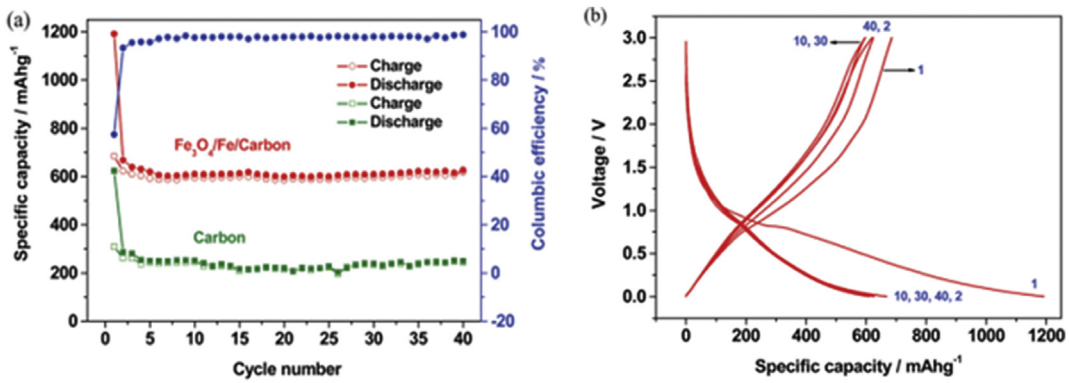

Fig. 2. (a) Cycling stability and (b) discharge–charge profiles of Fe_3O_4/Fe/carbon composite electrodes (adapted from Ref. [7]).

anode and demonstrated high reversible capacity, rapid charging, and discharging capability. An elevated capacity of 785 mAh g^{-1} was attained at 1C discharge–charge rate and was maintained up to 500 cycles. Furthermore, the electrode sustained a capacity of 190 mAh g^{-1} at 60 °C, indicating its potential to be fully charged in 1 min.

3.1.2. *Carbon-coated Fe_3O_4 tubular structures*

A tube-shaped structure was fabricated from carbon-coated Fe_3O_4 by Han et al. [14] using a MoO_3 nanorod as a hard template. Then, this template was removed and the structure was further modified with an optimized carbon nanocoating. The overall structure was not only hierarchical (built of smaller structural elements, which have their own structures) but also porous with a large surface area. The results of using this tabular structure as an anode for half of a Li-ion cell showed improved electronic conductivity, stable electrode–electrolyte interface, and a high degree of cycling performance with a specific capacity of 1020 mAh g^{-1} at 200 mA g^{-1} after 150 cycles. Furthermore, at a current density of 1000 mA g^{-1}, a capacity of 840 mAh g^{-1} was maintained subsequent to 300 cycles without any capacity loss.

3.1.3. *Uniform hierarchical Fe_3O_4 hollow spheres*

Ma et al. [15] established a solvothermal approach to fabricate extremely uniform hierarchical Fe_3O_4 hollow spheres. The synthesis procedure was composed of two major steps (Fig. 3): (1) uniform hierarchical Fe-containing precursor hollow spheres were manufactured using a single-pot solvothermal method using $Fe(NO_3)_3 \cdot 6H_2O$, glycerol, isopropanol, and water; (2) the Fe-glycerate precursor was annealed in nitrogen to convert it to a highly crystalline structure. The discharge capacities of the hierarchical Fe_3O_4 hollow sphere electrode were 992, 853, 716, 548, and 457 mAh g^{-1} at current densities of 1, 2, 4, 8, and 10 A g^{-1}.

3.1.4. *Bacteria inspired composites*

A biologically inspired approach was reported in Ref. [16], where a micro-/nanostructured-Fe_3O_4-carbon/GF hybrid was used as a LIB anode. The synthetic process (Fig. 4) comprised culture of *E scherichia coli* on the GF, which was then treated with methanol to increase permeability. Next, the *E. coli* was subjected to a medium containing 0.1 M $FeCl_3$, and finally, the mixture was annealed in argon. The resulting anode displayed a high

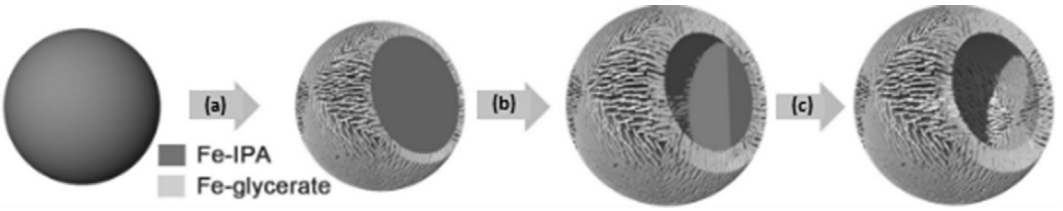

Fig. 3. The synthesis of the Fe-glycerate hollow sphere. (a) Deposition of Fe-glycerate nanosheets on the surface of the Fe-IPA solid spheres. (b) Growth of the nanosheets. (c) Formation of the hierarchical Fe-glycerate hollow sphere (adapted from Ref. [15]). IPA, isopropanol.

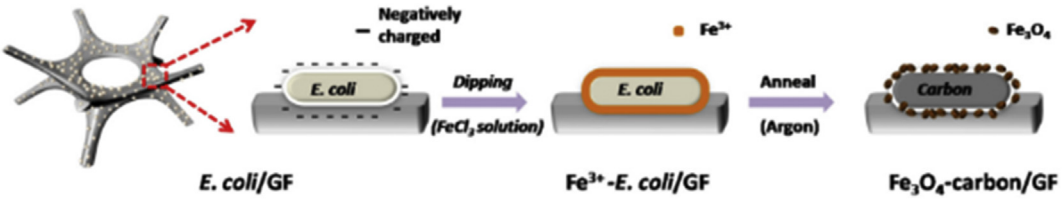

Fig. 4. Using *E. coli* in fabricating a Fe_3O_4-inspired anode [16].

reversible capacity of 1112 mAh g^{-1} at a current density of 100 mA g^{-1}, even past 200 cycles.

4. Fe_3O_4 composites

4.1. Fabrication of Fe_3O_4 composites

4.1.1. One-dimensional hierarchical Fe_3O_4/carbon nanofiber nanocomposites

Jiang et al. used a solvothermal technique and thermal annealing to synthesize one-dimensional hierarchical Fe_3O_4/carbon nanofiber (CNF) nanocomposites (Fig. 5) [17]. This approach allowed integrating Fe_3O_4 nanoparticles with highly conductive CNFs, which act as a supportive matrix for dispersing Fe_3O_4 nanoparticles. This resulted in a greater surface area and exceptional electrical conductivities of the composite. Furthermore, this design allowed easy penetration of the electrolyte into the porous CNF network. This, in turn, led to the augmentation of the contact area between the electrolyte and active materials. It is worth noting that individual CNFs provided a rapid and efficient electron transfer pathway, consequently, the Fe_3O_4/CNF nanostructures displayed a reversible discharge capacity of 684 mAh g^{-1} after 55 cycles.

4.1.2. Fe_3O_4–graphene nanocomposites

Ultrafine Fe_3O_4 nanoparticles were uniformly anchored onto graphene substrates to construct Fe_3O_4–graphene nanocomposites through a hydrothermal process [18]. As an anode material for LIB, the nanocomposites displayed superior initial discharge and charge capacities of 1456 and 739.9 mAh g^{-1}, respectively, at a high current density of 500 mA g^{-1}. In addition, the charge capacity was maintained at 698.3 mAh g^{-1} after 200 cycles.

4.1.3. High capacity Fe_3O_4 nanorod/graphene composites

Another approach used Fe_3O_4 nanorod/graphene composites [19]. The synthesis process for these composites consisted of two steps: (1) FeOOH/graphene composites were first synthesized through uniform dispersion of FeOOH nanorods on graphene sheets, and (2) annealing in an argon atmosphere to form Fe_3O_4/graphene composites. One of the reasons for using graphene is to employ it as a reducing agent during the different phases of the composite manufacturing. The synthesized Fe_3O_4 nanorods were shown to have electrical contact with the graphene sheet, which also contributed to improving the overall electrochemical performance of the composite, with a reversible specific capacity of 1155 mAh g^{-1}.

4.1.4. Three-dimensional Fe_3O_4 quantum dots/graphene aerogel materials

The particle sizes of quantum dots (QDs) are smaller than other nanomaterials in at least one dimension. They also possess an excellent cycling stability and demonstrate high capabilities in terms of electronic/ionic conductivity,

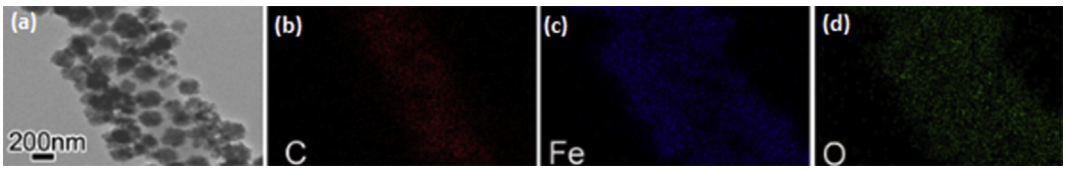

Fig. 5. (a) Transmission electron microscope (TEM) image of Fe_3O_4/CNFs and corresponding mapping of (b) carbon, (c) iron, and (d) oxygen elements (adapted from Ref. [17]).

specific surface area, and volume effect. They also show a lower number of defects in the crystal structure. QDs were used to manufacture a Fe_3O_4 QDs/graphene aerogel via a hydrothermal reaction followed by a heat treatment procedure [20]. The addition of graphene enhanced the electronic and mechanical properties of the aerogel. However, the resulting electrode displayed a high irreversible capacity loss, which was likely to be caused by the large electrochemical interfacial values resulting from Li^+ storage.

4.1.5. Yolk and sac approach

Zhang et al. [21] sandwiched a heterogeneous Fe_3O_4–Fe_3C core–shell nanoparticle inside a hollow carbon nanospindle to form a yolk–sac structure (Fig. 6). This design created an internal void space that could accommodate volume changes of Fe_3O_4. In addition, using the Fe_3C shell restricted Fe_3O_4 dissolution. Overall, these added features enhanced the electrochemical characteristics of the composite, as evident from its reversible capacity (1128.3 mAh g^{-1} at 500 mA g^{-1}), rate capacity (604.8 mAh g^{-1} at 2000 mA g^{-1}), and cycling life (1120.2 mAh g^{-1} at 500 mA $g^{-1}$for 100 cycles). The authors claimed that their design was the best Fe_3O_4-based anode material ever reported for LIBs.

5. Stable Fe_3O_4-metal oxide combinations

Transition metal oxides possess higher electrochemical capacities than carbon anodes. However, they suffer from both low volume variation and inferior conductivity [22]. One strategy aimed to benefit from electrochemical capacity of high transition metal oxides by using their substrates as current collectors. These substrates were integrated with electrode materials via a coating procedure. Unfortunately, this approach did not show much potential as the substrates suffered from low flexibility, heavy weight, and not being environmentally friendly. To address these challenges, TiO_2–α-Fe_2O_3 core–shell arrays were introduced. This configuration had multiple advantages, including large interfacial area, reduction of the diffusion pathways for electronic and ionic transport, induction of a positive synergistic effect, superior rate capability, large reversible capacity, and exceptional cycle performance. Therefore, this approach could represent an immense potential as an efficient anode material for Li storage. This idea was further extended in Taberna et al. [23], where an electrochemically assisted template growth of Cu-nanorods onto a current collector was followed by electrochemical plating of Fe_3O_4. A sixfold increase in power density over typical electrodes

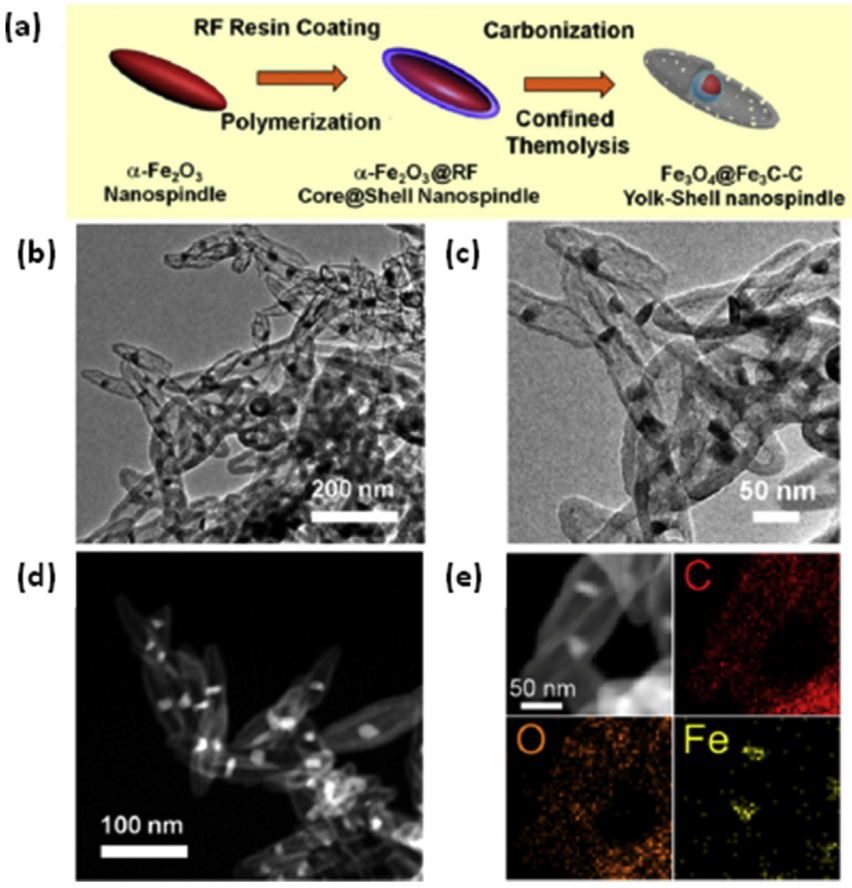

Fig. 6. (a) The fabrication of the Fe_3O_4@Fe_3C–C yolk shell nanospindles. (b, c) TEM images, (d) Scanning electron microscope (SEM) image, and (e) TEM-Energy dispersive spectrometer (EDS) mapping [21].

Table 1
Pros and cons of Fe_3O_4 fabrication methods.

Technique	Advantages	Disadvantages
Electrospinning	High surface area to volume ratio, tunable porosity, superior capacity retention	Low tensile properties, poor durability
Sol–gel reaction	High voltage plateau, reduced lithium plating on electrode	Modest charge capacity, many step process
Graphene foam	Rapid charging and discharging, very good reproducibility, and consistency	Tedious manufacturing process
Carbon-coated tubular structures	Stable electrode–electrolyte interface, excellent cycling performance	Expensive, rare raw materials, different scale up
Hollow spheres	Excellent discharge capacities	Many step process
Bacteria inspired composites	Very good charge density and capacity	Not environmentally friendly
Fe_3O_4/CNF	Excellent electrical conductivity	Safety issues with carbon nanotubes
Fe_3O_4/graphene	Superior initial discharge and charge capacities	Expensive
Fe_3O_4 nanorod/graphene	Very high reversible specific capacity	Rare raw materials
Fe_3O_4 quantum dots/graphene aerogel	Excellent electronic and ionic conductivity	High irreversible capacity loss
Yolk–sac nanoparticles	Superior cycle life and reversible capacity	Tedious to create hollow carbon nanospindle, inconsistent nanoparticle size
Fe_3O_4 metal oxides	High electrochemical capacities	Low volume variation, inferior conductivity, inflexible, high density

was observed, while conserving the overall discharge time. Furthermore, the capacity at the 8C rate was 80% of the total capacity after 100 cycles. However, a large hysteresis between charge and discharge was detected.

6. Fabrication technique comparisons

Many routes have been described to fabricate Fe_3O_4 anodes whether in fiber form, nanostructures, composites, or other forms. Each process has its advantages and disadvantages depending on the comparison and property that is being optimized. Table 1 highlights some of the positive and negative characteristics of each manufacturing technique.

7. Applications of Fe_3O_4 microstructures in LIBs

Designing new Fe_3O_4 electrodes for LIBs could have a large impact in the future. Recently, the Li-air battery has gained momentum as it could deliver 5–10 times greater energy density as compared with classical LIBs. The theoretical specific energy density of a Li-air battery is 5200 Wh kg^{-1}, whereas that of a LIB is only 150 Wh kg^{-1} [24]. Fe_3O_4 is a putative material for Li-air batteries owing to its oxygen reduction catalytic activity [25]. However, one of the challenges toward Fe_3O_4 deployment in Li-air batteries is the large volume changes and severe aggregation of the Fe_3O_4 particles that could take place during the charge–discharge cycling phases. In our research works, we reported novel pagoda-like Fe_3O_4 microstructures, which were produced by a microemulsion-mediated hydrothermal process, and then used as oxygen reduction catalysts in the air electrodes of lithium-air batteries [25]. This strategy has been shown to enhance the cell ability to have an initial discharge capacity of 1429 mAh g^{-1} at 1.5–4.5 V and 100 mA g^{-1}. In another work, we prepared mace-like Fe_3O_4 nanostructures using a solvothermal method in cyclohexane/Triton X-100/*n*-amyl alcohol/water system [26]. The results of charge–discharge tests based on these nanostructures exhibited a high discharge capacity of 1427 mAh g^{-1} in ambient air. However, the battery still suffered from low cyclic performance, likely due to the accumulation of partially oxidized products. To address this issue, advanced analysis is being performed to quantify the reasons behind the poor cycling ability.

8. Conclusions

The application of Fe_3O_4 anode for Li batteries is gaining popularity. There are several approaches for the production of Fe_3O_4 anodes, such as electrospinning and sol–gel processes. There are also multiple strategies for Fe_3O_4 anode design, including using nanostructures with diverse morphologies (sphere, tube, and foam) and in combination with graphene or another metal. Among the currently available methods, the electrochemical properties of Fe_3O_4/carbon-based electrode materials seem to outperform other methods. However, much progress in electrochemical performance through rational design is still needed to revolutionize the automobile and energy industry.

Acknowledgments

This research was supported by the National Natural Science Foundation of China (No. 51674262).

References

[1] J.B. Goodenough, K.-S. Park, J. Am. Chem. Soc. 135 (2013) 1167–1176.
[2] S. Shawn Lee, T.H. Kim, S. Jack Hu, W.W. Cai, J.A. Abell, in: ASME 2010 International Manufacturing Science and Engineering Conference, American Society of Mechanical Engineers, 2010, pp. 541–549.
[3] D. Deng, Energy Sci. Eng. 3 (2015) 385–418.
[4] B. Yu, M. Wang, H. Sun, F. Zhu, J. Han, G. Bhat, RSC Adv. 7 (2017) 41929–41935.
[5] Z. Wang, L. Zhou, X.W. David Lou, Adv. Mater. 24 (2012) 1903–1911.

[6] H. Campos, J. Ayala, C. Valdes, J.G. Parsons, M. Alcoutlabi, MOJ Polym. Sci. 2 (2018), https://doi.org/10.15406/mojps.2018.02.00045.
[7] X. Zhao, D. Xia, K. Zheng, ACS Appl. Mater. Interfaces 4 (2012) 1350–1356.
[8] N. Bhardwaj, S.C. Kundu, Biotechnol. Adv. 28 (2010) 325–347.
[9] J. Li, Y. Wu, M. Yang, Y. Yuan, W. Yin, Q. Peng, Y. Li, X. He, J. Am. Ceram. Soc. 100 (2017) 5460–5470.
[10] L. Ji, O. Toprakci, M. Alcoutlabi, Y. Yao, Y. Li, S. Zhang, B. Guo, Z. Lin, X. Zhang, ACS Appl. Mater. Interfaces 4 (2012) 2672–2679.
[11] J. Luo, J. Liu, Z. Zeng, C.F. Ng, L. Ma, H. Zhang, J. Lin, Z. Shen, H.J. Fan, Nano Lett. 13 (2013) 6136–6143.
[12] S. Yang, Y. Sun, L. Chen, Y. Hernandez, X. Feng, K. Müllen, Sci. Rep. 2 (2012) 427.
[13] R.W. Johnson, A. Hultqvist, S.F. Bent, Mater. Today 17 (2014) 236–246.
[14] F. Han, L. Ma, Q. Sun, C. Lei, A. Lu, Nano Res. 7 (2014) 1706–1717.
[15] F.-X. Ma, H. Hu, H.B. Wu, C.-Y. Xu, Z. Xu, L. Zhen, X.W. Lou, Adv. Mater. 27 (2015) 4097–4101.
[16] N. Zhang, C. Chen, X. Yan, Y. Huang, J. Li, J. Ma, D.H.L. Ng, Electrochim. Acta 223 (2017) 39–46.
[17] F. Jiang, S. Zhao, J. Guo, Q. Su, J. Zhang, G. Du, J. Nanoparticle Res. 17 (2015) 348.
[18] S.-S. Chen, X. Qin, Nano 10 (2015) 1550081.
[19] Y. Wang, A. Pan, Int. J. Electrochem. Sci. 12 (2017) 2506–2519.
[20] Y. Wang, Y. Jin, Y. Duan, M. Jia, Ionics 23 (2017) 2005–2011.
[21] J. Zhang, K. Wang, Q. Xu, Y. Zhou, F. Cheng, S. Guo, ACS Nano 9 (2015) 3369–3376.
[22] Y. Luo, J. Luo, J. Jiang, W. Zhou, H. Yang, X. Qi, H. Zhang, H.J. Fan, D.Y.W. Yu, C.M. Li, T. Yu, Energy Environ. Sci. 5 (2012) 6559–6566.
[23] P.L. Taberna, S. Mitra, P. Poizot, P. Simon, J.-M. Tarascon, Nat. Mater. 5 (2006) 567–573.
[24] M.A. Rahman, X. Wang, C. Wen, J. Appl. Electrochem. 44 (2014) 5–22.
[25] H. Lv, R. Jiang, Y. Li, X. Zhang, J. Wang, Ceram. Int. 41 (2015) 8843–8848.
[26] H. Lv, R. Jiang, X. Zhang, J. Wang, Aust. J. Chem. 69 (2016) 683–688.